

Pre-stack seismic reflection inversion with basis pursuit

Postdoc fellow: Rui Zhang

Advisor: Dr. Mrinal Sen and Dr. Sanjay Srinivasan

THE UNIVERSITY OF TEXAS AT AUSTIN

JACKSON

SCHOOL OF GEOSCIENCES

Outline

- Motivation
- Formulations
- Synthetic tests
- Field data
- Discussions
- Conclusions

THE UNIVERSITY OF TEXAS AT AUSTIN

JACKSON

SCHOOL OF GEOSCIENCES

Motivation

- Post-stack to pre-stack
- Acoustic to elastic
- Improved resolution

GEOPHYSICS, Vol. 76, No. 6 (DECEMBER-DECEMBER 2011), P. R147-R158, 12 FIGS
10.1190/GEO2011-0081

Seismic sparse-layer reflectivity inversion using basis pursuit decomposition

Rui Zhang¹ and John Castagna²

ABSTRACT

A basis pursuit inversion of seismic reflection data for reflection coefficients is introduced as an alternative method of incorporating a priori information in the seismic inversion process. The inversion is accomplished by building a dictionary of functions representing reflectivity patterns and constituting the seismic trace as a superposition of these patterns. Basis pursuit decomposition finds a sparse number of reflection responses that sum to form the seismic trace. When the dictionary of functions is chosen to be a wedge-model of reflection coefficient pairs convolved with the seismic wavelet, the resulting reflectivity inversion is a sparse-layer inversion, rather than a sparse-spike inversion. Synthetic tests suggest that a sparse-layer inversion using basis pursuit can better resolve thin beds than a comparable sparse-spike inversion. Application to field data indicates that sparse-layer inversion results in the potentially improved detectability and resolution of some thin layers and reveals apparent stratigraphic features that are not readily seen on conventional seismic sections.

INTRODUCTION

In conventional seismic deconvolution, the seismogram is convolved with a wavelet inverse filter to yield band-limited reflectivity. The output reflectivity is band limited to the original frequency band of the data so as to avoid blowing up noise at frequencies with little or no signal. It has long been established (e.g., Riel and Berkhout, 1985) that sparse seismic inversion methods can produce output reflectivity solutions that contain frequencies that are not contained in the original signal without necessarily magnifying noise at those frequencies. It is well known (e.g., Tarantola, 2004)

that applying valid constraints in seismic inversion can stably increase the bandwidth of the solution.

However, incorporation of the a priori information in the reflectivity inversion of seismic traces can be problematic. A common way of incorporating prior knowledge is to build a starting model biased by that information and to let the inversion process perturb the initial starting model and converge to a solution (e.g., Cooke and Schuster, 1983). The individual layers represented in the starting model can have hard or soft constraints assigned. This kind of method can work very well when the starting model is close to the correct solution. Typically, the starting model is obtained by spatially interpolating well logs along selected horizons. Unfortunately, these horizons must be picked on the original seismic data. If waveform interference patterns change laterally, horizon picks on a constant portion of a waveform (typically chosen to be peaks, troughs, or zero crossings) can be in error, resulting in an incorrect starting model and a potentially erroneous inversion. Similarly, if velocities and/or impedances for the inversion interval change laterally in a manner different from that resulting from the interpolation procedure, interpolated well logs may again be significantly in error, and the inverse process may converge to the wrong minimum. These problems may be ameliorated with a Monte Carlo approach, but such an approach cannot correct the fundamental nonuniqueness of the process that may cause minimums other than the correct one to have similar errors. A means of biasing the results toward expected reflectivity patterns is needed without relying on possibly erroneous manual interpretations or spatial interpolations.

Nguyen and Castagna (2010) used matching pursuit decomposition (MPD) to decompose a seismic trace into a superposition of reflectivity patterns observed in and derived from existing well control. Matching pursuit decomposition (1) correlates a wavelet dictionary against a seismogram and finds the location, scale (i.e., center frequency), and amplitude of the best-fit wavelet, (2) subtracts the best-fit wavelet and records its characteristics in a table, and (3) repeats the processes on the residual trace until the residual energy falls below a selected threshold. For spectral decomposition,

Manuscript received by the Editor 14 March 2011; revised manuscript received 24 July 2011; published online 22 December 2011.
¹University of Texas, Jackson School of Geosciences, Institute for Geophysics, Austin, Texas, USA. E-mail: rzhang@mail.utexas.edu.
²University of Houston, Department of Earth and Atmospheric Sciences, Houston, Texas, USA. E-mail: jcastagna@uh.edu.
© 2011 Society of Exploration Geophysicists. All rights reserved.

R147

Downloaded 26 Feb 2012 to 129.116.220.97. Redistribution subject to SEG license or copyright; see Terms of Use at <http://library.seg.org/>

Outline

- Motivation
- Formulations
- Synthetic tests
- Field data
- Discussions
- Conclusions

THE UNIVERSITY OF TEXAS AT AUSTIN

JACKSON

SCHOOL OF GEOSCIENCES

Formulations

Aki & Richard

$$R(\theta) = \frac{1}{2} (1 + \tan^2 \theta) \frac{\Delta V_p}{V_p} - \frac{4\beta^2}{\alpha^2} \sin^2 \theta \frac{\Delta V_s}{V_s} - \left[\frac{1}{2} \tan^2 \theta - 2\beta^2 \right] \frac{\Delta \rho}{\rho}$$

$$R(\theta, t) = \frac{1}{2} (1 + \tan^2 \theta) \frac{\Delta V_p(t)}{V_p(t)} - \frac{4\beta^2}{\alpha^2} \sin^2 \theta \frac{\Delta V_s(t)}{V_s(t)} - \left[\frac{1}{2} \tan^2 \theta - 2\beta^2 \right] \frac{\Delta \rho(t)}{\rho(t)}$$

$$R_p(t) = \frac{\Delta V_p(t)}{V_p(t)} \quad C_p = \frac{1}{2} (1 + \tan^2 \theta)$$

$$R_s(t) = \frac{\Delta V_s(t)}{V_s(t)} \quad C_s = -\frac{4\beta^2}{\alpha^2} \sin^2 \theta$$

$$R_\rho(t) = \frac{\Delta \rho(t)}{\rho(t)} \quad C_\rho = -\left(\frac{1}{2} \tan^2 \theta - 2\beta^2 \right) \sin^2 \theta$$

β/α is background V_s/V_p ratio

THE UNIVERSITY OF TEXAS AT AUSTIN

JACKSON

SCHOOL OF GEOSCIENCES

Formulations

$$\begin{bmatrix} R_{pp}(t, \theta_1) \\ R_{pp}(t, \theta_2) \\ \vdots \\ R_{pp}(t, \theta_N) \end{bmatrix} = \begin{bmatrix} C_p(t, \theta_1) & C_s(t, \theta_1) & C_\rho(t, \theta_1) \\ C_p(t, \theta_2) & C_s(t, \theta_2) & C_\rho(t, \theta_2) \\ \vdots & \vdots & \vdots \\ C_p(t, \theta_N) & C_s(t, \theta_N) & C_\rho(t, \theta_N) \end{bmatrix} \times \begin{bmatrix} R_p(t) \\ R_s(t) \\ R_\rho(t) \end{bmatrix},$$

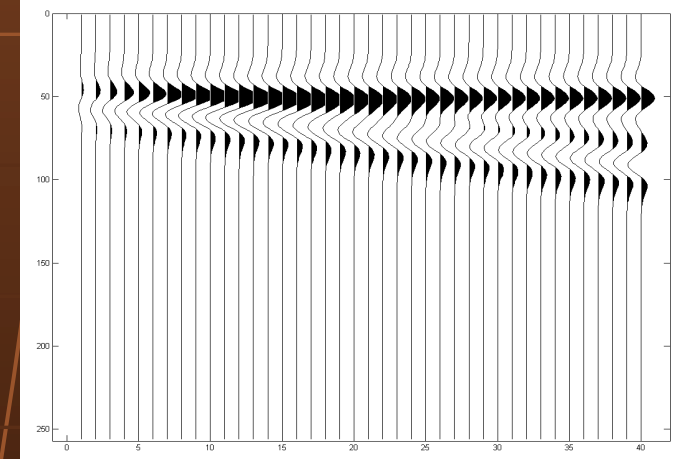
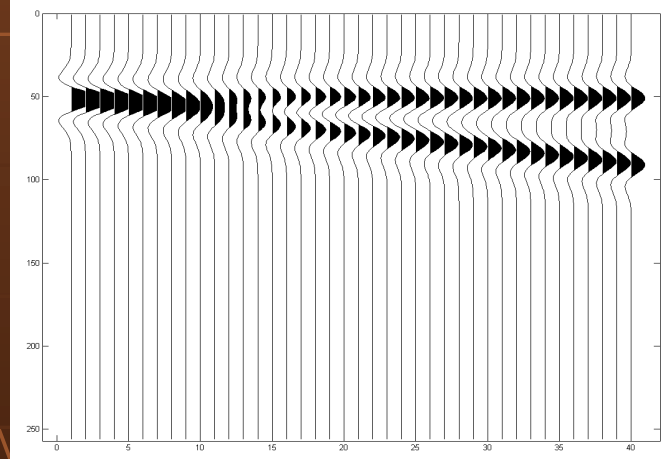
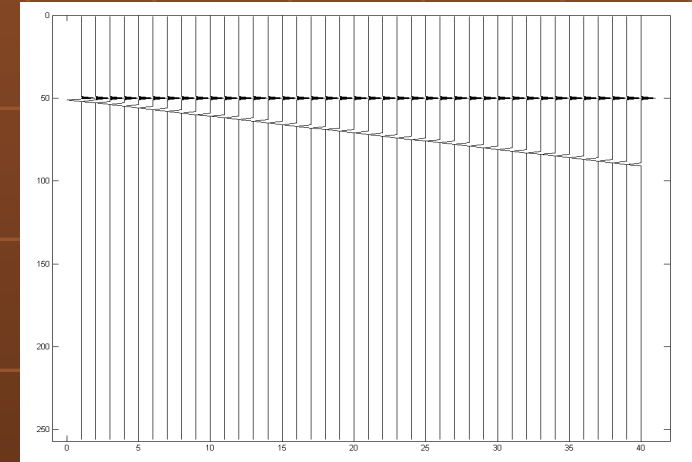
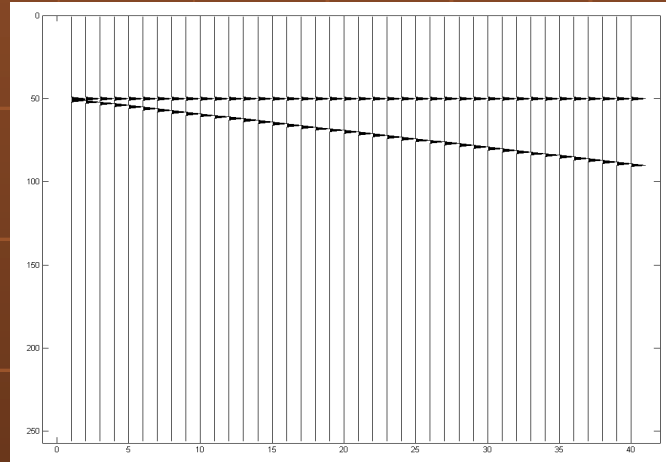
$$\begin{bmatrix} S_{pp}(t, \theta_1) \\ S_{pp}(t, \theta_2) \\ \vdots \\ S_{pp}(t, \theta_N) \end{bmatrix} = \begin{bmatrix} W_p(t, \theta_1) & W_s(t, \theta_1) & W_\rho(t, \theta_1) \\ W_p(t, \theta_2) & W_s(t, \theta_2) & W_\rho(t, \theta_2) \\ \vdots & \vdots & \vdots \\ W_p(t, \theta_N) & W_s(t, \theta_N) & W_\rho(t, \theta_N) \end{bmatrix} \times \begin{bmatrix} R_p(t) \\ R_s(t) \\ R_\rho(t) \end{bmatrix}.$$

Formulations

$$\left[\begin{array}{c} | \\ \hline | \\ \hline | \end{array} \right] = a \left[\begin{array}{c} | \\ \hline | \\ \hline | \end{array} \right] + b \left[\begin{array}{c} | \\ \hline | \\ \hline | \end{array} \right]$$

Even

Odd



Wedge reflectivity

Wedge seismic response

Formulations

$$R_p(t) = \sum_{n=1}^N \sum_{m=1}^M (aep_{n,m} * r_e(t, m, n, \Delta t) + bop_{n,m} * r_o(t, m, n, \Delta t))$$

$$R_s(t) = \sum_{n=1}^N \sum_{m=1}^M (aes_{n,m} * r_e(t, m, n, \Delta t) + bos_{n,m} * r_o(t, m, n, \Delta t))$$

$$R_\rho(t) = \sum_{n=1}^N \sum_{m=1}^M (aep_{n,m} * r_e(t, m, n, \Delta t) + bop_{n,m} * r_o(t, m, n, \Delta t))$$

$$\begin{bmatrix} R_p(t) \\ R_s(t) \\ R_\rho(t) \end{bmatrix} = \begin{bmatrix} r_e & r_o & 0 & 0 & 0 & 0 \\ 0 & 0 & r_e & r_o & 0 & 0 \\ 0 & 0 & 0 & 0 & r_e & r_o \end{bmatrix} \times \begin{bmatrix} aep \\ bop \\ aes \\ bos \\ aep \\ bop \end{bmatrix}$$

Formulations

b

A

x

$$\begin{bmatrix} S_{pp}(t, \theta_1) \\ S_{pp}(t, \theta_2) \\ \vdots \\ S_{pp}(t, \theta_N) \end{bmatrix} = \begin{bmatrix} W_p(t, \theta_1) & W_s(t, \theta_1) & W_\rho(t, \theta_1) \\ W_p(t, \theta_2) & W_s(t, \theta_2) & W_\rho(t, \theta_2) \\ \vdots & \vdots & \vdots \\ W_p(t, \theta_N) & W_s(t, \theta_N) & W_\rho(t, \theta_N) \end{bmatrix} \times \begin{bmatrix} [r_e, r_o] & 0 & 0 \\ 0 & [r_e, r_o] & 0 \\ 0 & 0 & [r_e, r_o] \end{bmatrix} \times \begin{bmatrix} aep \\ bop \\ aes \\ bos \\ aep \\ bop \end{bmatrix}$$

Objective Function

L1 norm minimization least square solution

$$\min \|x\|_1$$

Subject to

$$\min \|b - A \times x\|_2$$

$$\min \left[\|b - A \times x\|_2 + \lambda \|x\|_1 \right]$$

Velocity

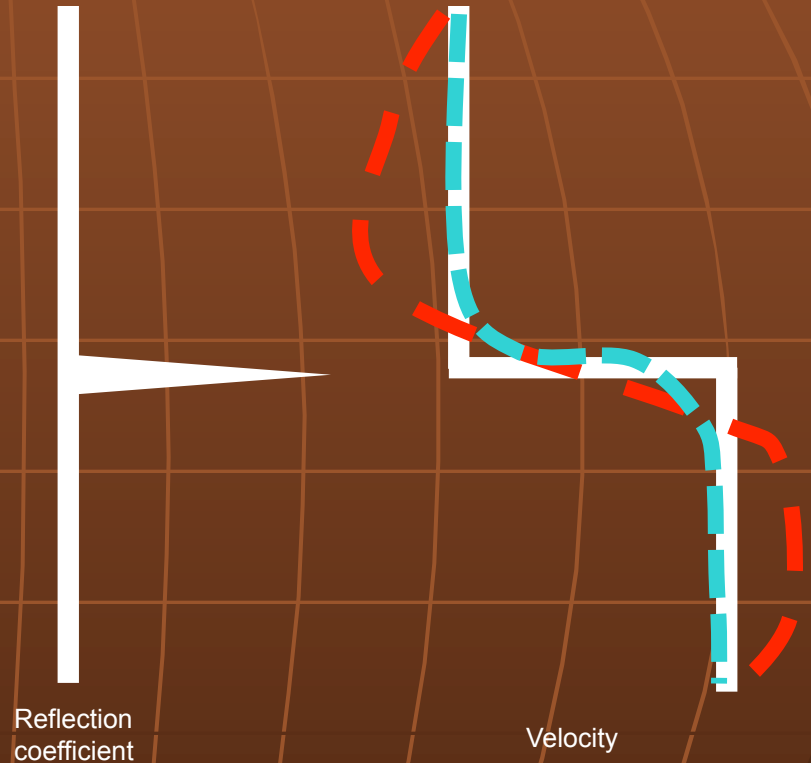
$$r_{\downarrow t} = \Delta V_{\downarrow t} / V_{\downarrow t} = \Delta \ln V_{\downarrow t}$$

$$\ln V_{\downarrow t} = \ln V_{\downarrow t}(0) + \int_0^t r_{\downarrow t} dt$$

$$V_{\downarrow t} = V_{\downarrow t}(0) e^{\int_0^t r_{\downarrow t} dt}$$

$r_{\downarrow t}$: Reflection coefficient

Velocity



- Real
- BPI
- Conventional

Outline

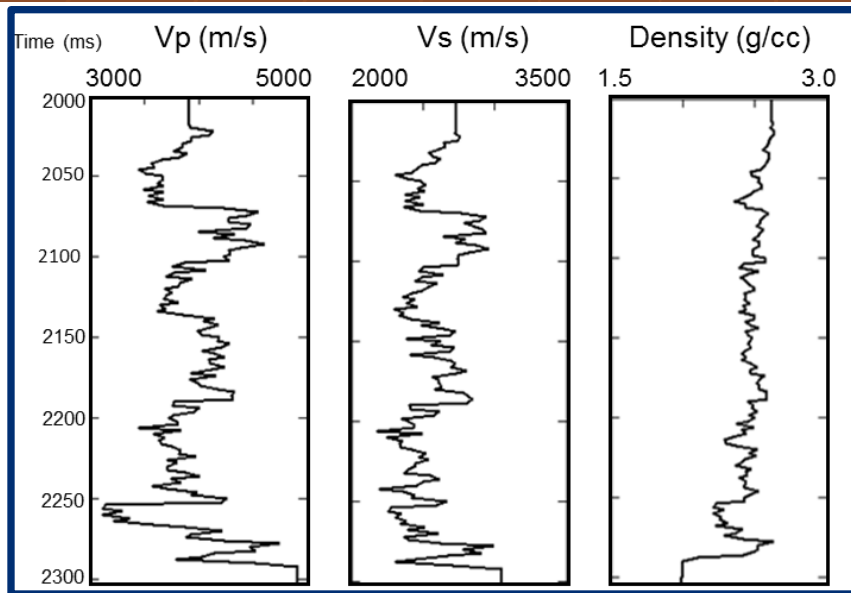
- Motivation
- Formulations
- Synthetic tests
- Field data
- Discussions
- Conclusions

THE UNIVERSITY OF TEXAS AT AUSTIN

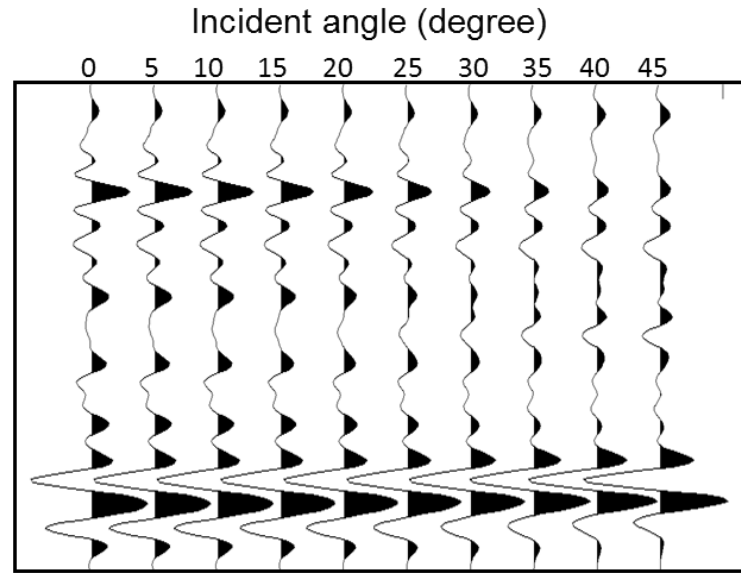
JACKSON

SCHOOL OF GEOSCIENCES

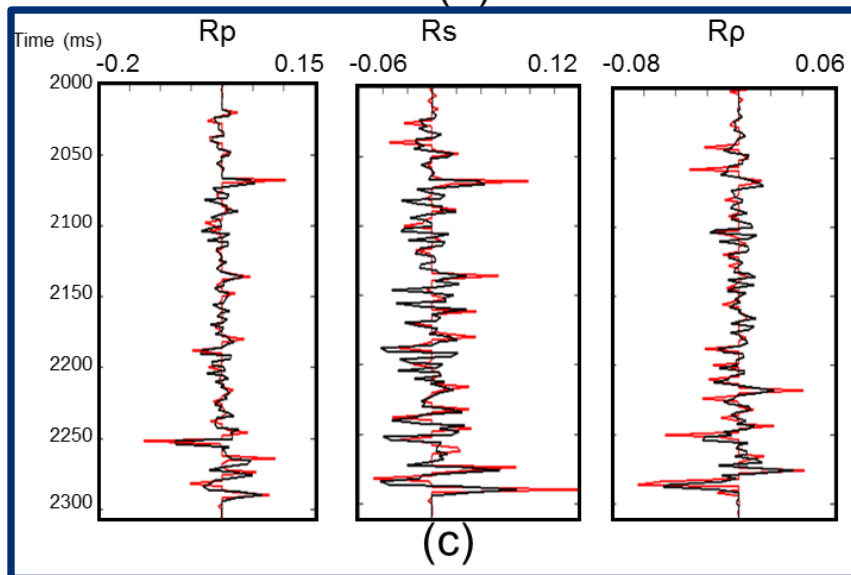
1D Synthetic tests



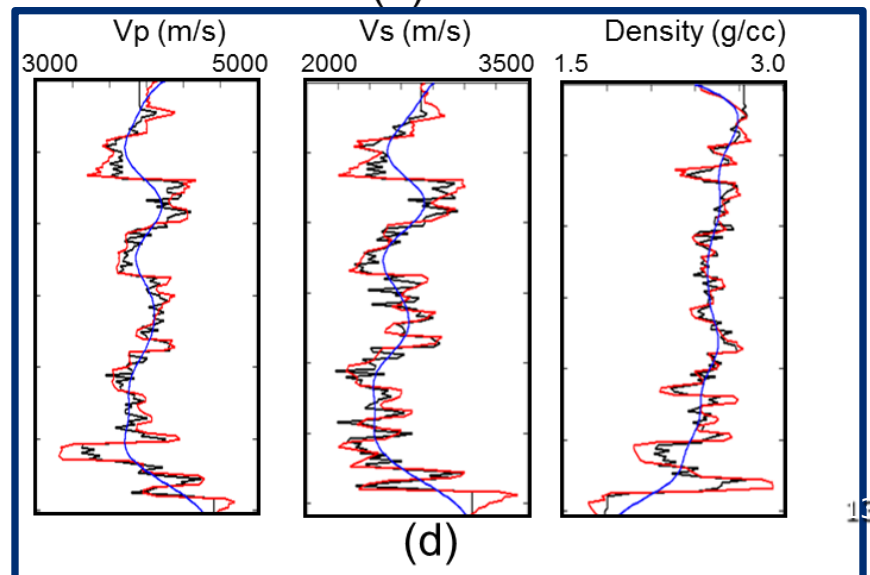
(a)



(b)

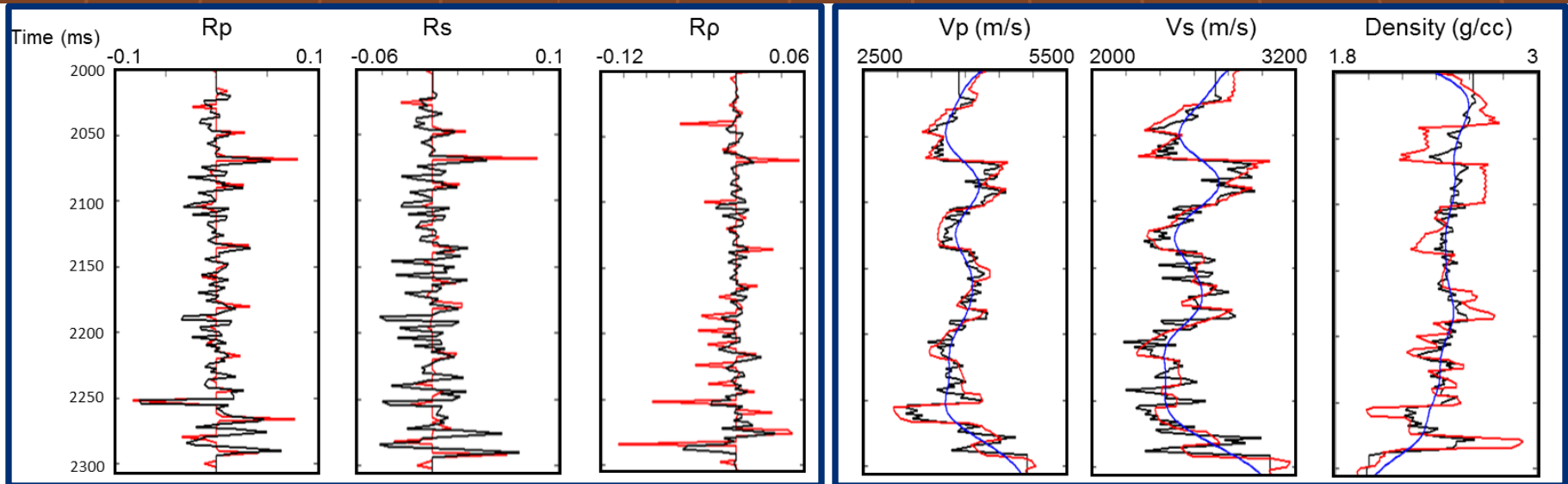


(c)



(d)

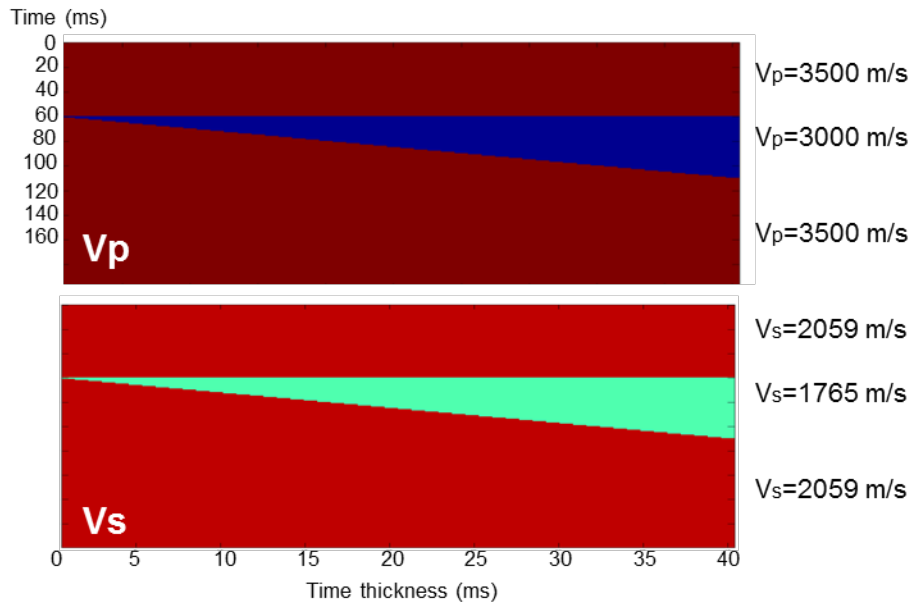
20% noise



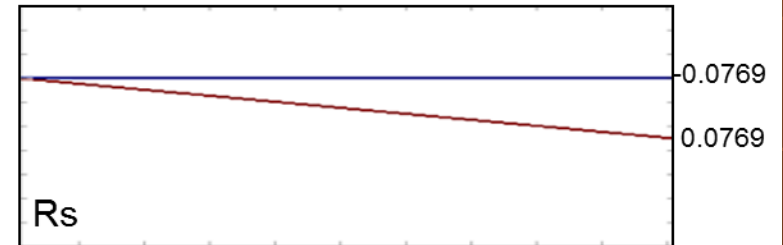
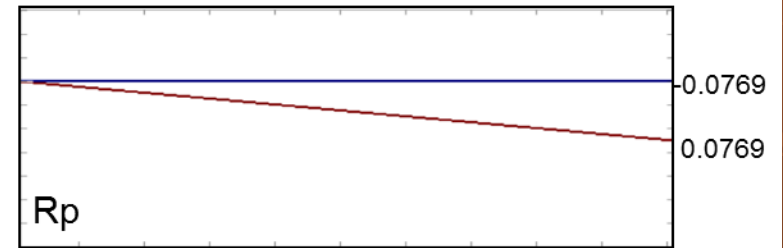
(a)

(b)

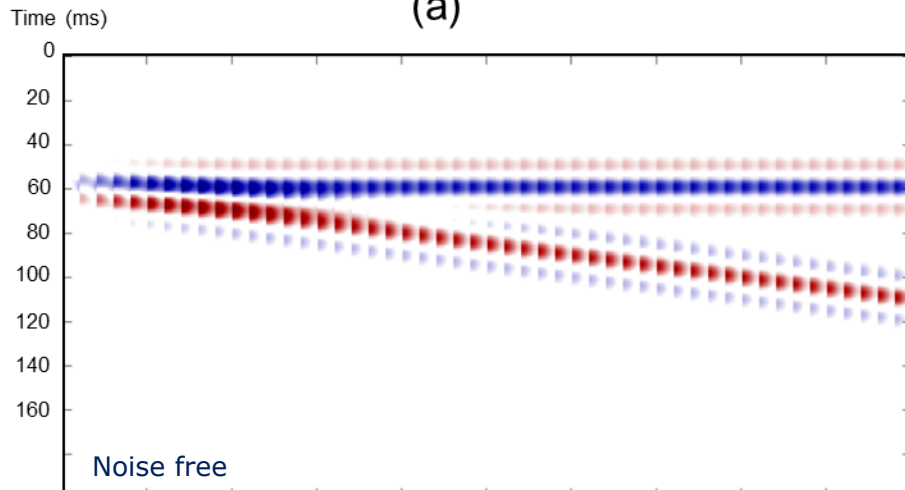
2D Synthetic tests



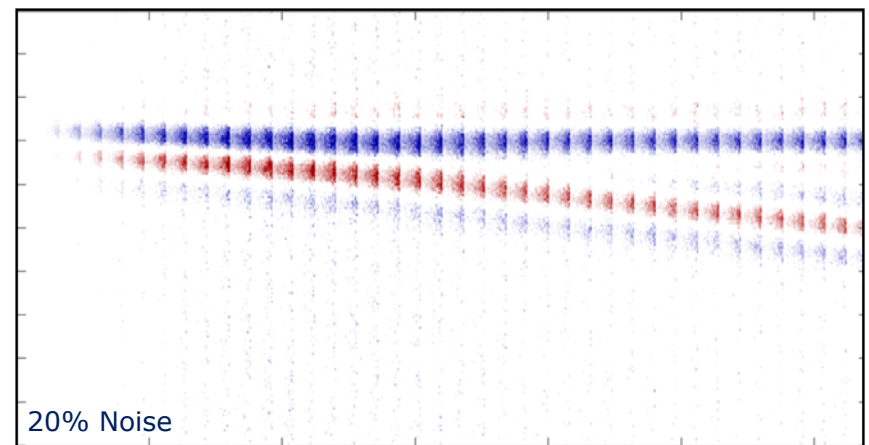
(a)



(b)



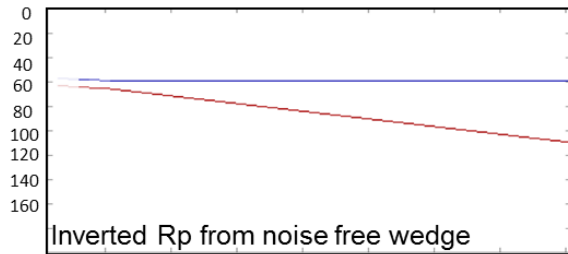
(c)



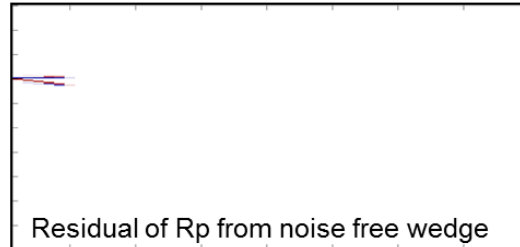
(d)

2D Synthetic tests

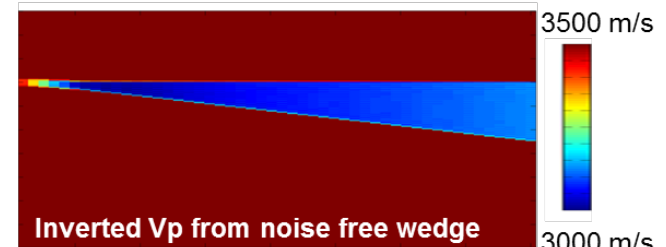
Time (ms)



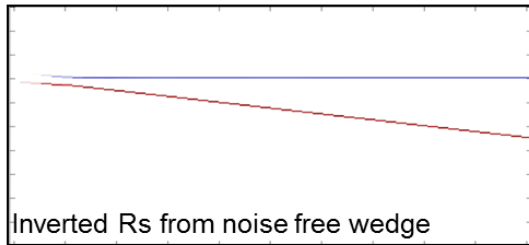
(a)



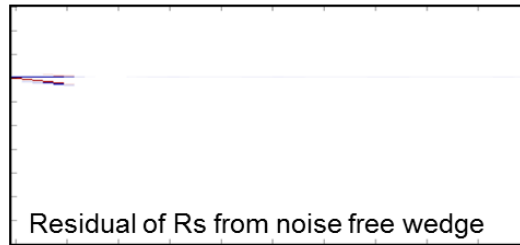
(b)



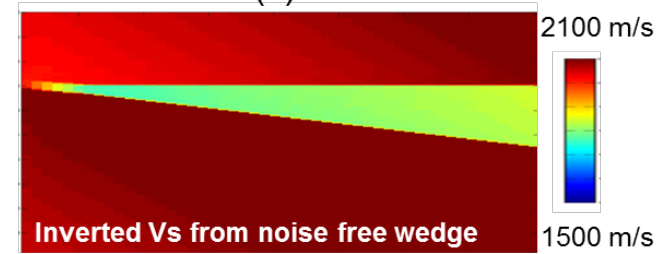
(c)



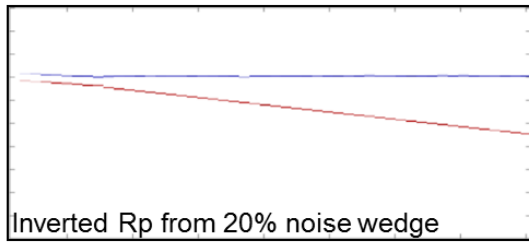
(d)



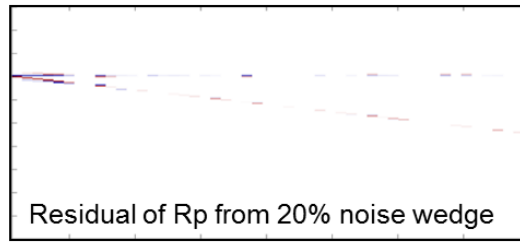
(e)



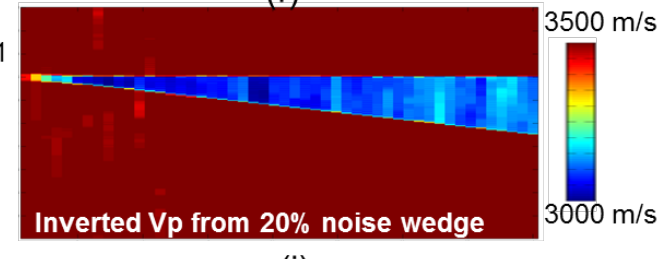
(f)



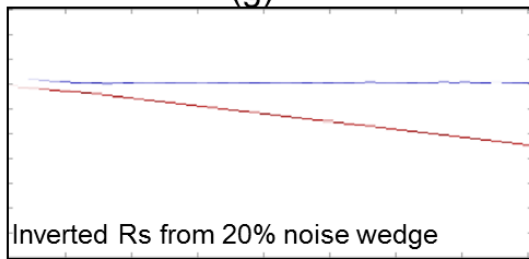
(g)



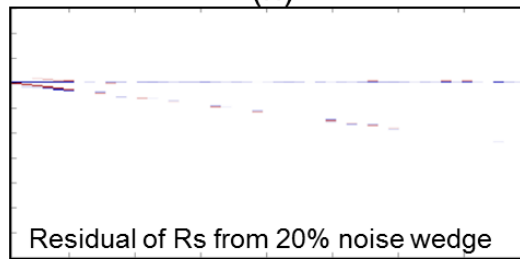
(h)



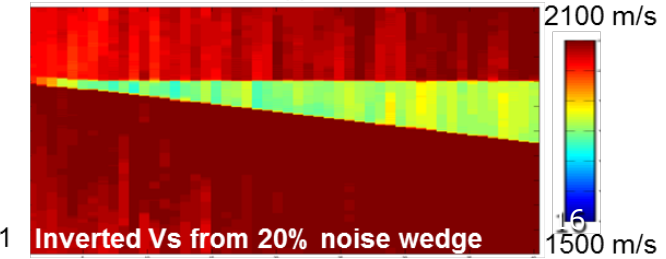
(i)



(j)



(k)



(l)

Outline

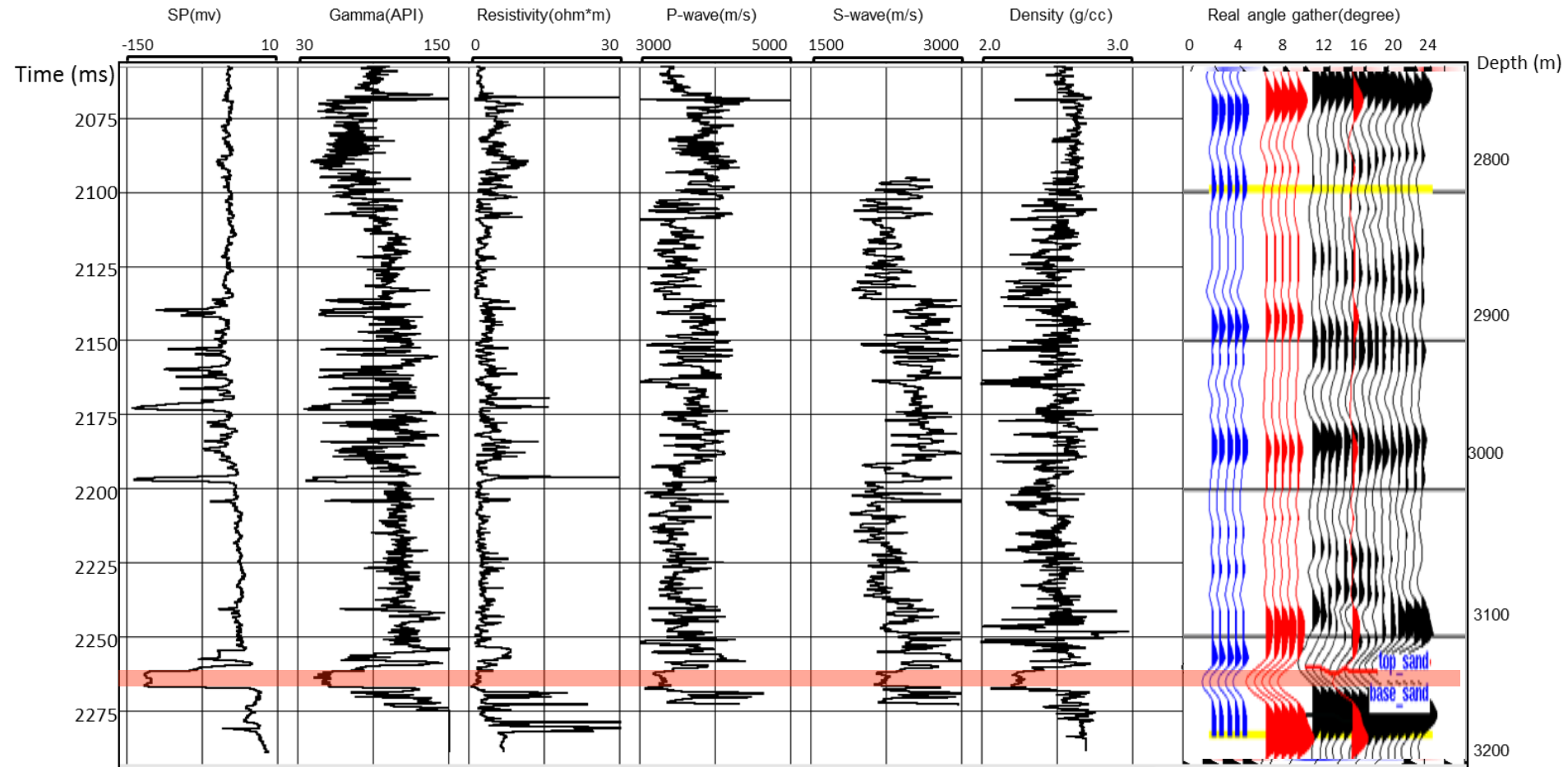
- Motivation
- Formulations
- Synthetic tests
- Field data
- Discussions
- Conclusions

THE UNIVERSITY OF TEXAS AT AUSTIN

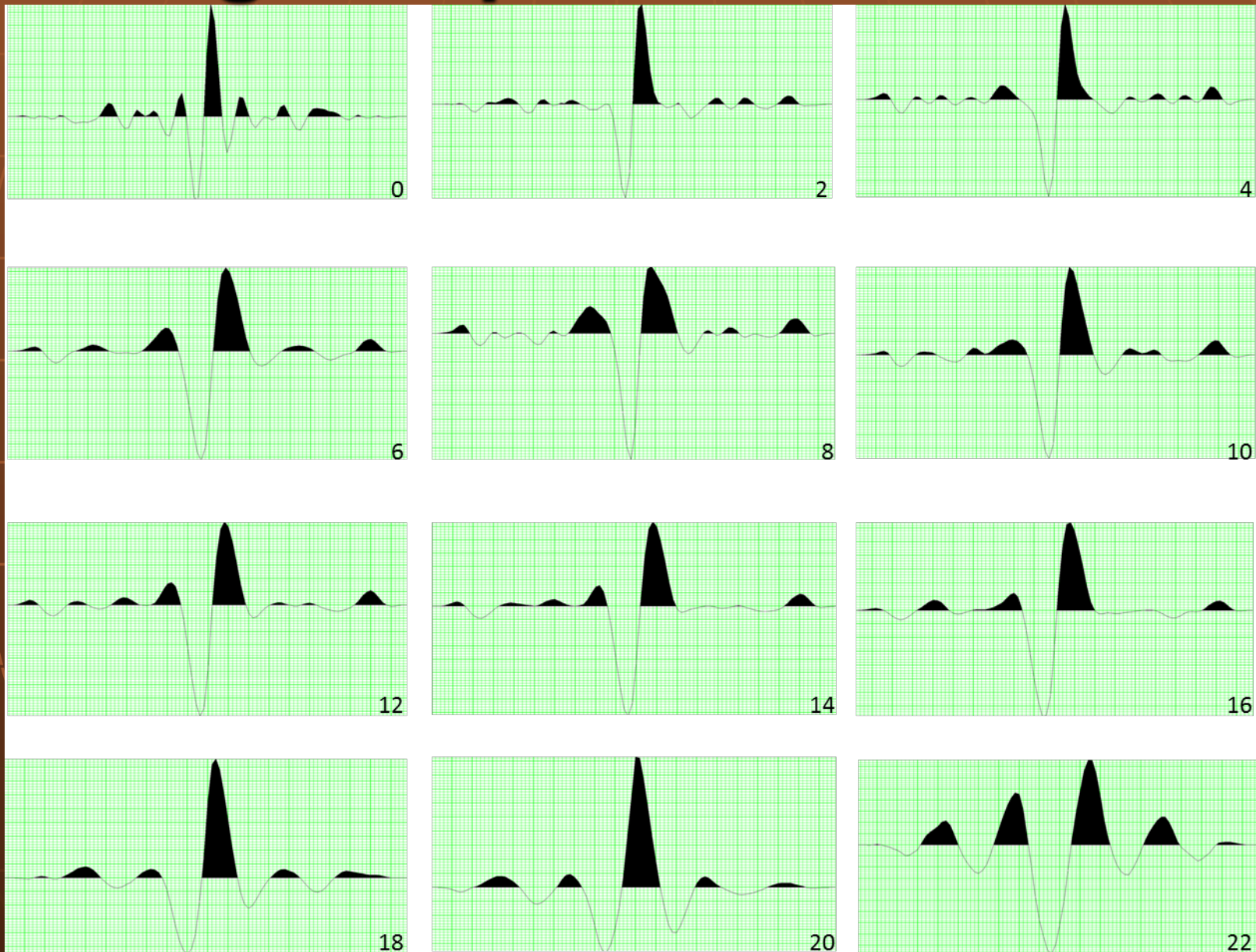
JACKSON

SCHOOL OF GEOSCIENCES

Seismic well "tie"



Angle dependent wavelets



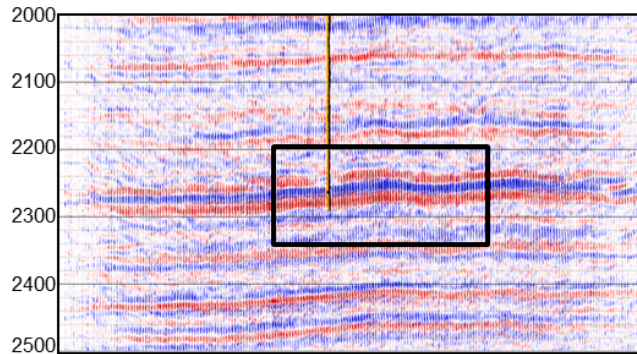
Inverted Reflection Coefficients

Pre-stack seismic

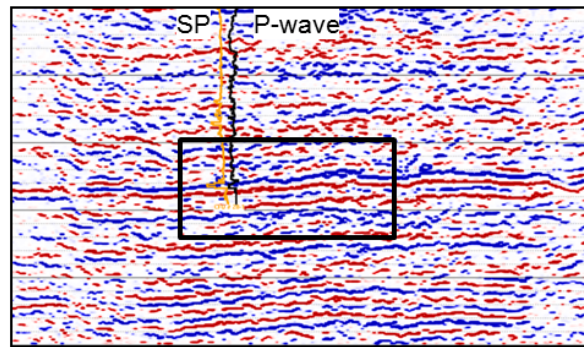
Inverted R_p

Inverted R_s

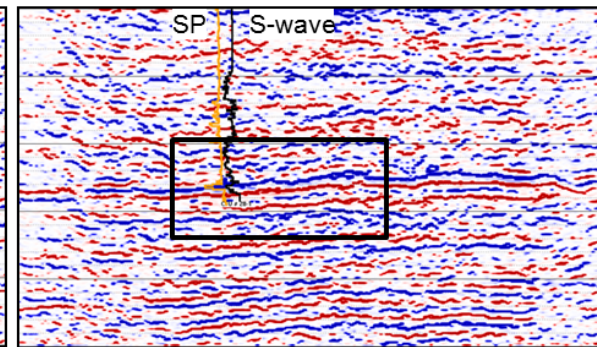
Time (ms)



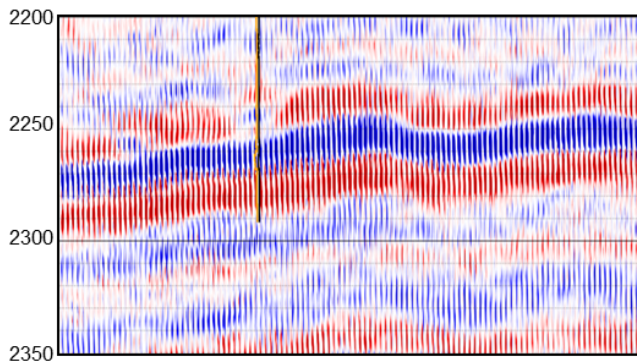
(a)



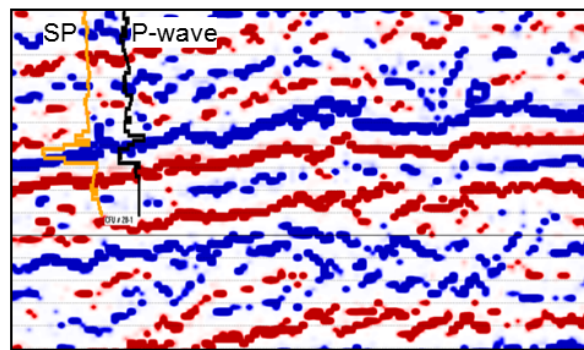
(b)



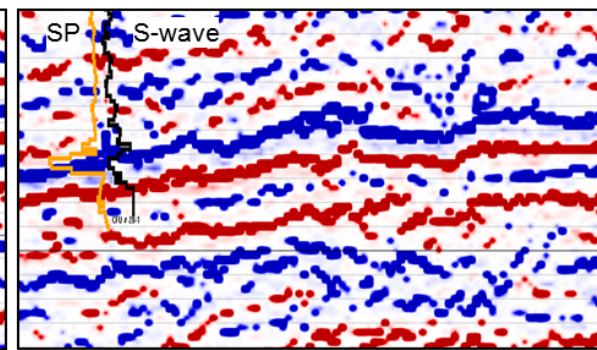
(c)



(d)



(e)



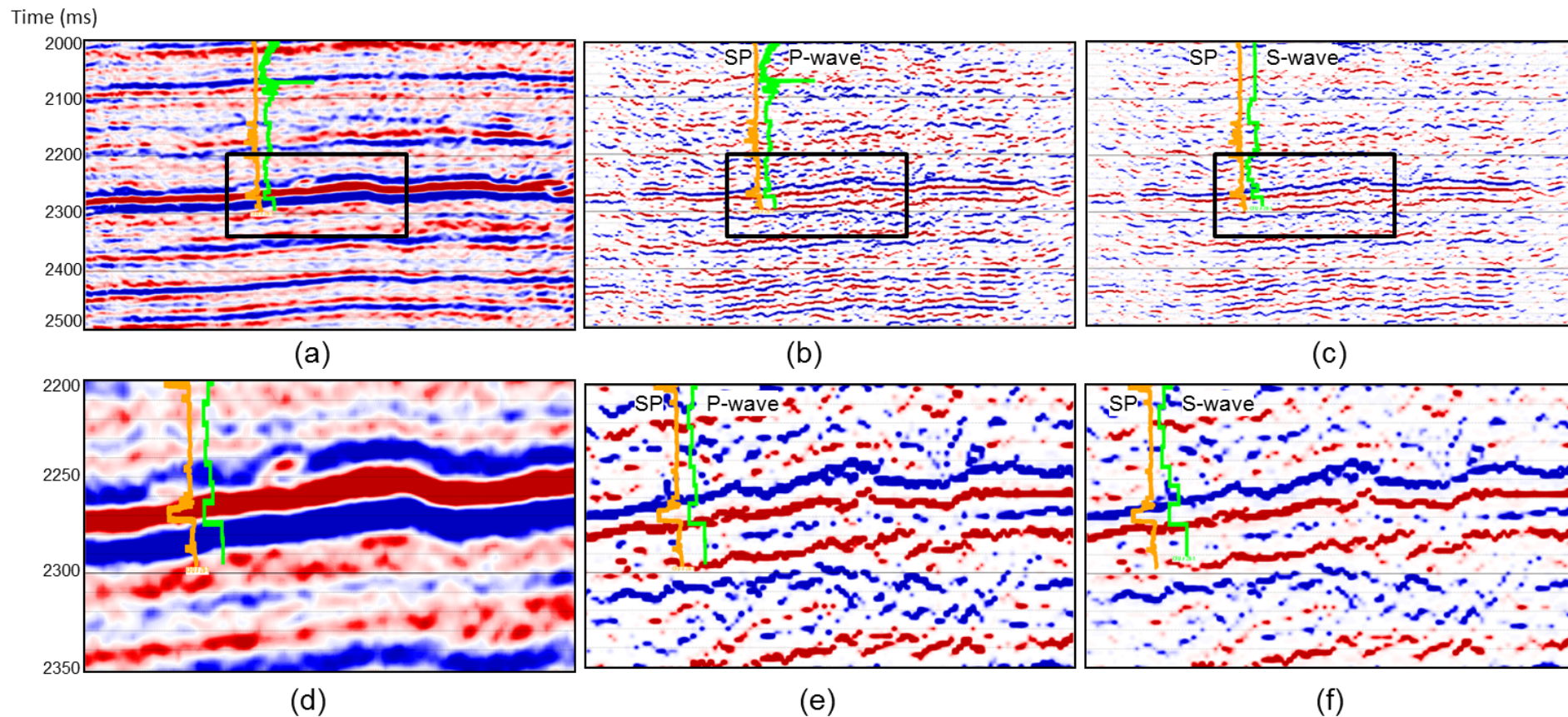
(f)

Inverted Reflection Coefficients

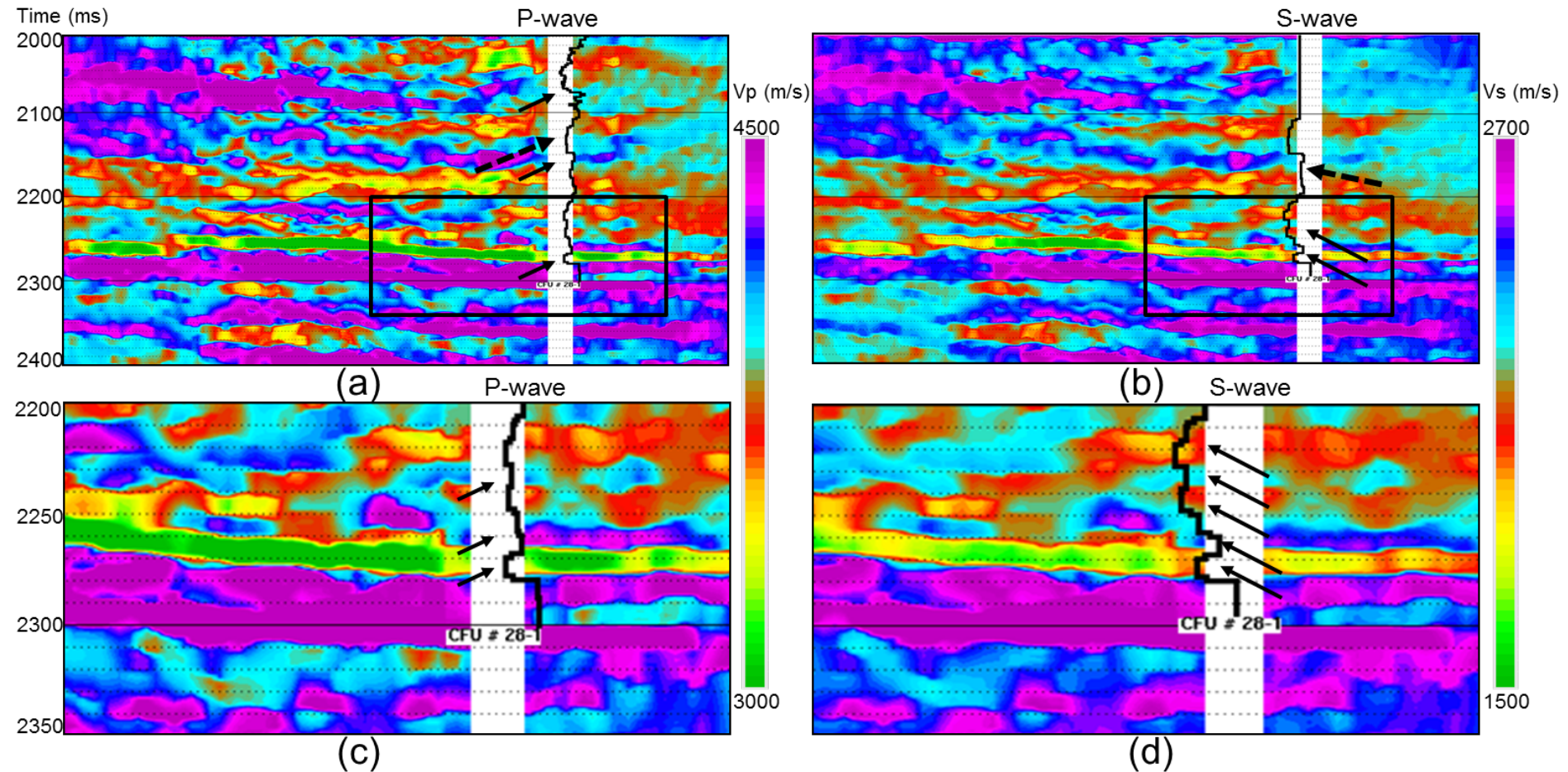
Post-stack seismic

Inverted R_p

Inverted R_s



Inverted Velocity

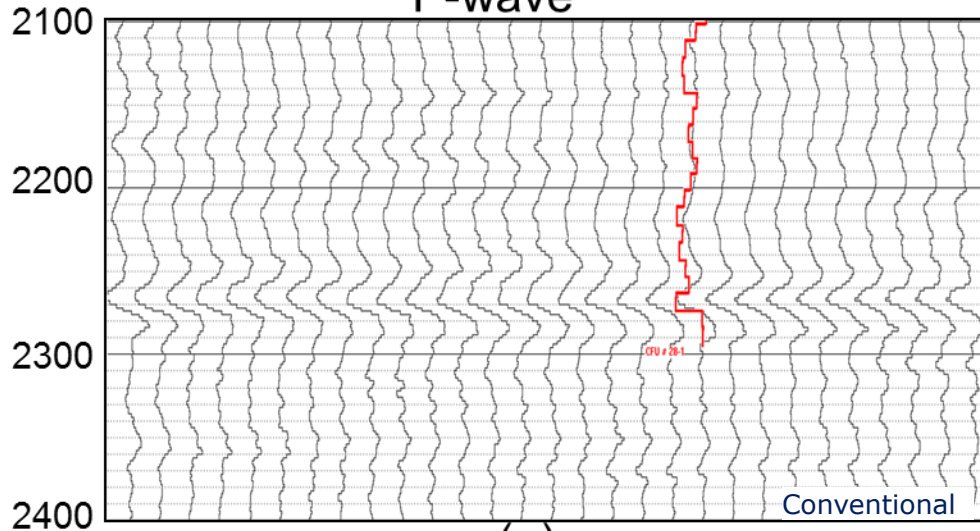


Inverted Velocity

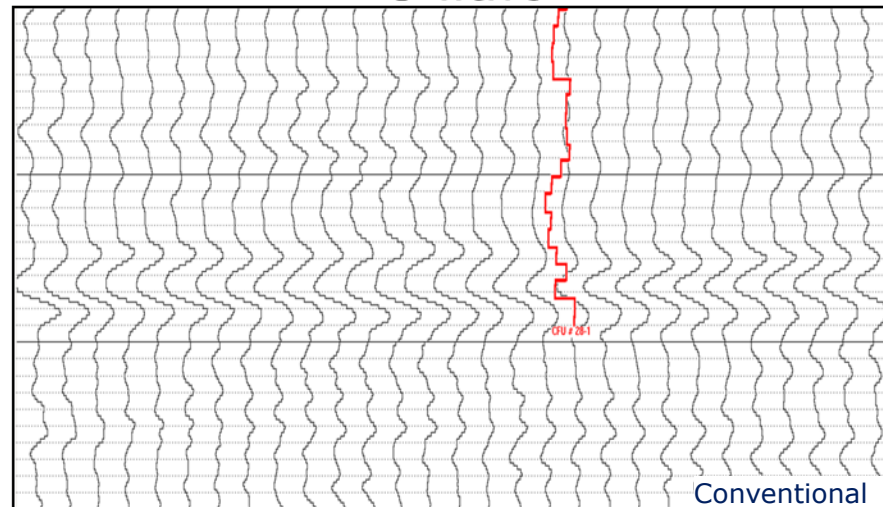
Time (ms)

P-wave

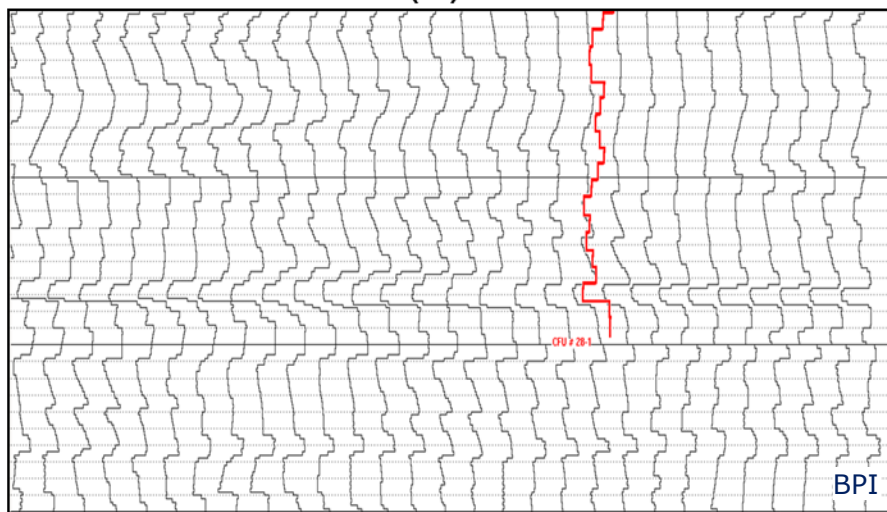
S-wave



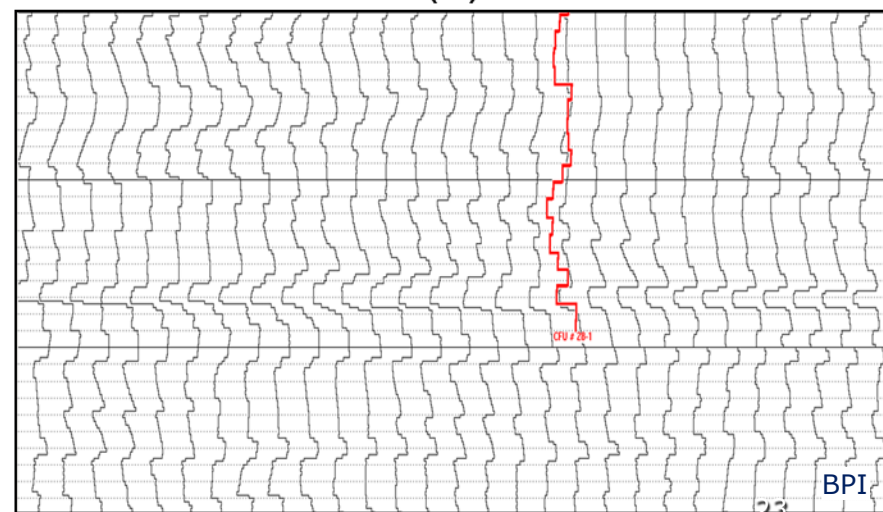
(a)



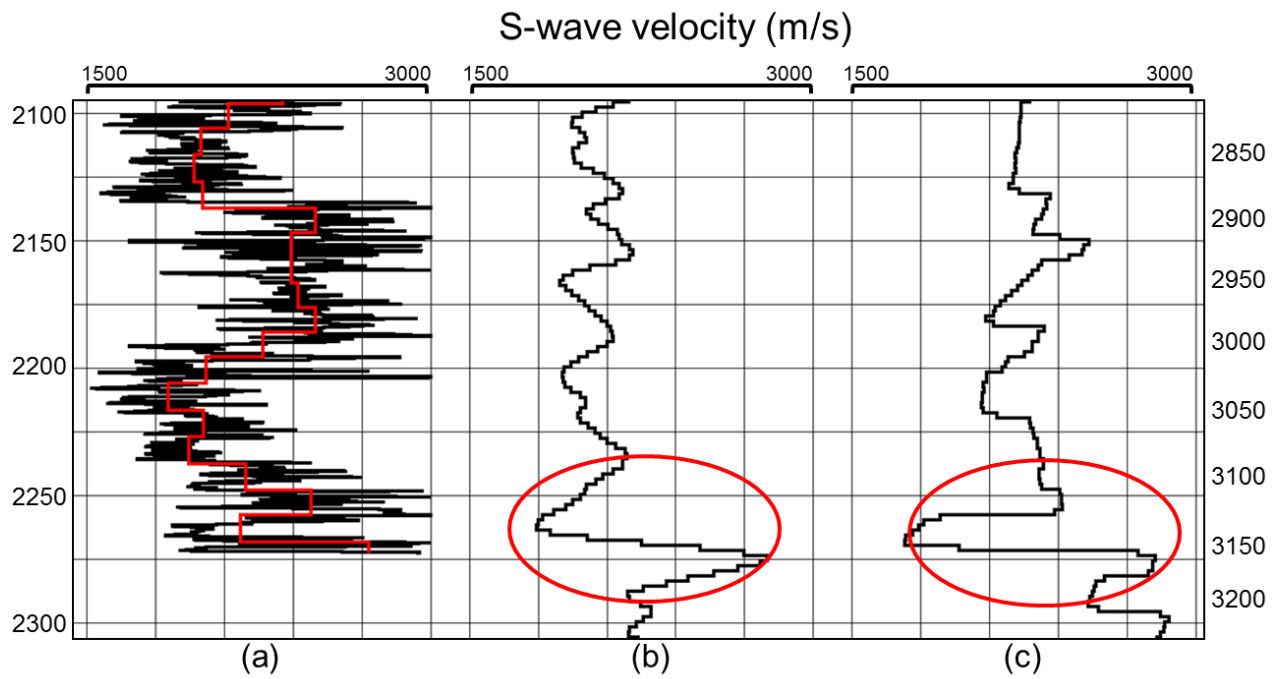
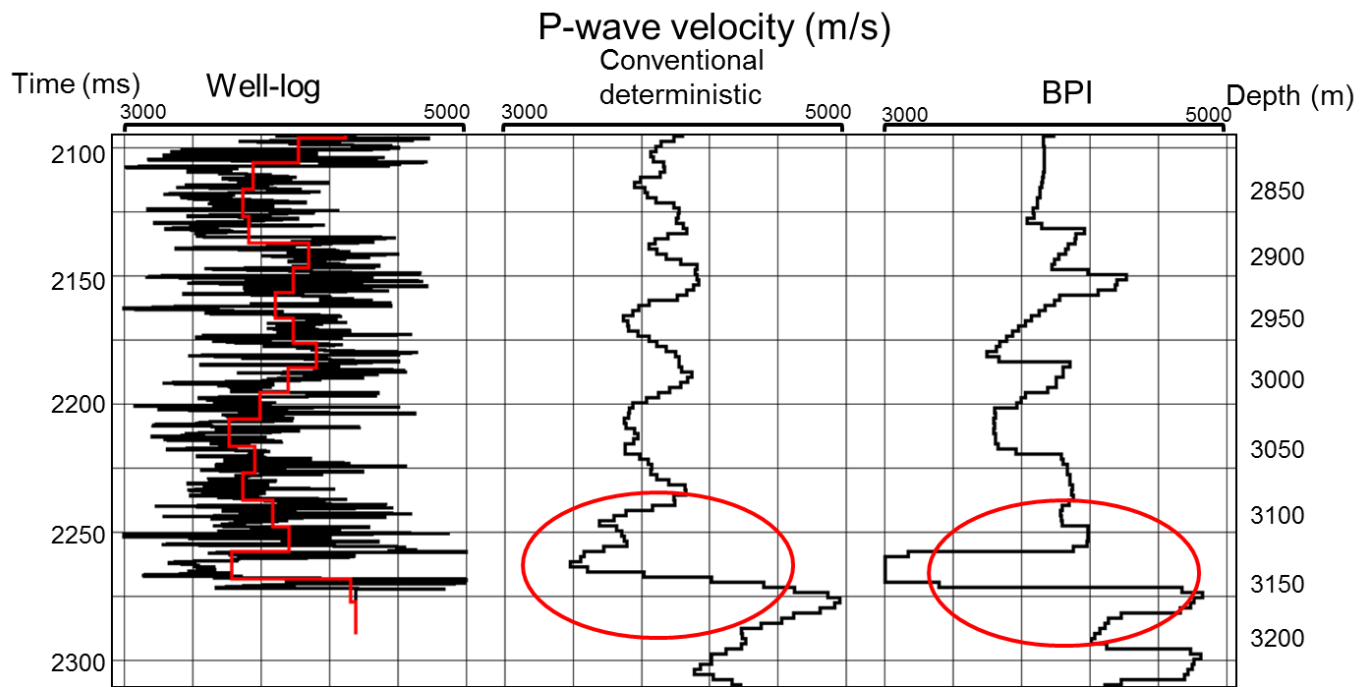
(b)



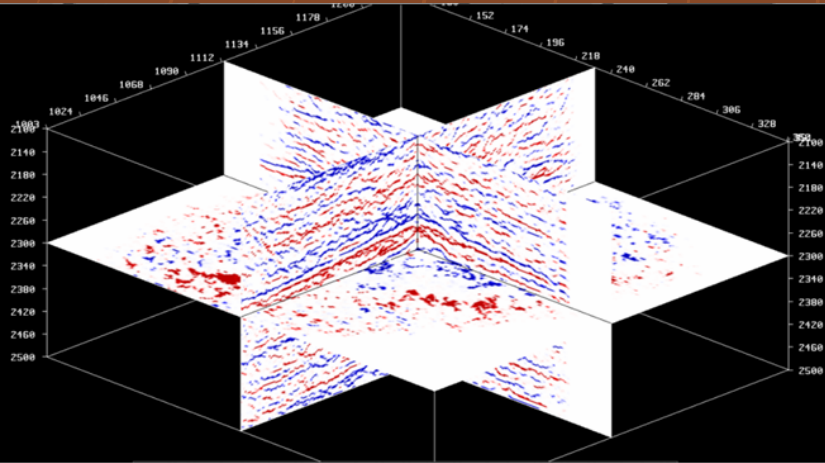
(c)



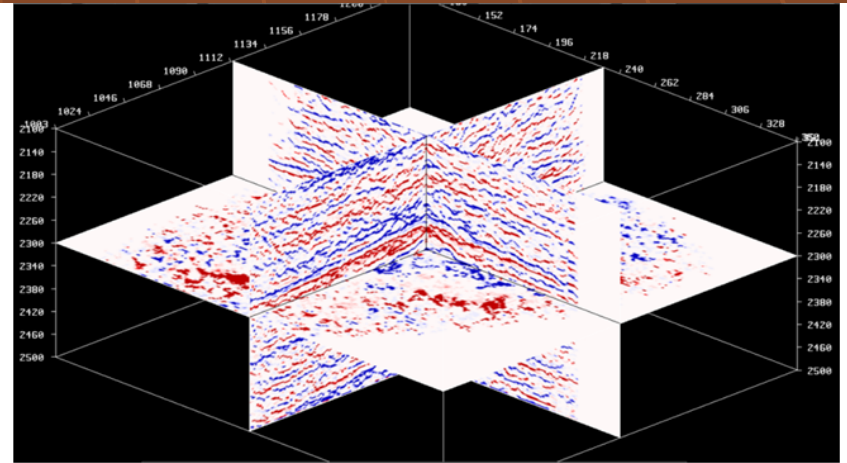
(d)



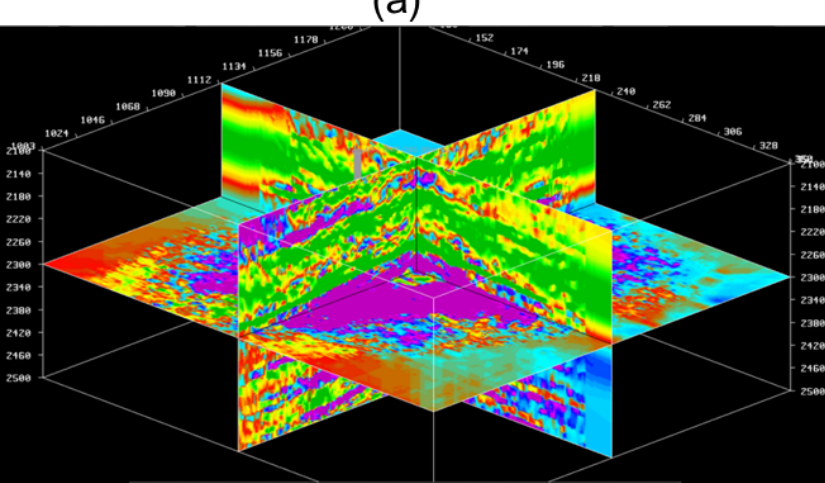
3D results



(a)



(b)

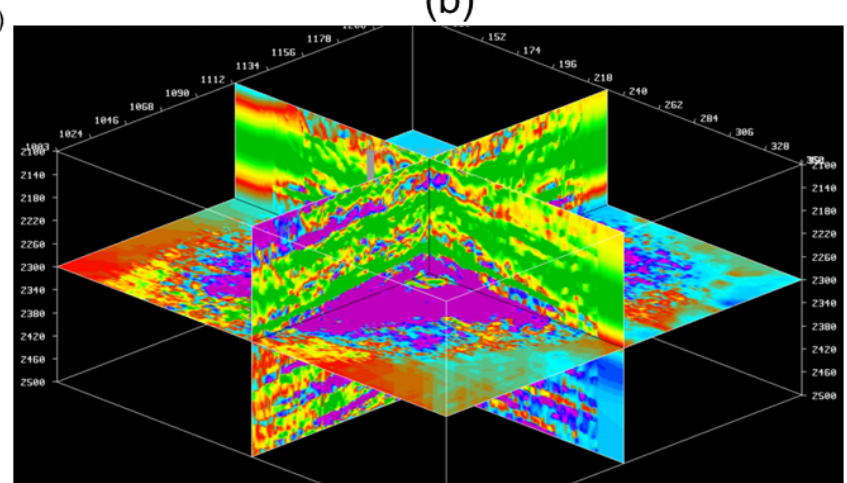


(c)

V_p (m/s)

4500

3000



(d)

V_s (m/s)

2700

1500

25

Discussions

- Perfect processing
- Offset-angle conversion
- Accommodation of non-stationary
- Angle range
- Pre-stack seismic well “tie”
- Initial model

Conclusions

- Spiky reflectivities R_p and R_s is initial model independent
- Blocky velocity V_p and V_s is initial model dependent
- Angle dependent wavelets can stabilize the results
- Two steps workflow can be QCed twice
- Blocky results enhance layer cake removing side lobes

Acknowledgements

- This work supported by Center for Frontiers of Subsurface Energy Security , an Energy Frontier Research Center funded by the U.S. Department of Energy, Office of Science, Office of Basic Energy Sciences under Award Number DE-SC0001114
- Dr. Susan D. Hovorka (BEG, GCCC) for providing data from Cranfield